

Anomalous decrease of the specific heat capacity at the electrical and thermal conductivity percolation threshold in nanocomposites

B.-W. Kim, S.-H. Park, and P. R. Bandaru

Citation: [Applied Physics Letters](#) **105**, 253108 (2014); doi: 10.1063/1.4905133

View online: <http://dx.doi.org/10.1063/1.4905133>

View Table of Contents: <http://scitation.aip.org/content/aip/journal/apl/105/25?ver=pdfcov>

Published by the [AIP Publishing](#)

Articles you may be interested in

[Evidence of percolation related power law behavior in the thermal conductivity of nanotube/polymer composites](#)
Appl. Phys. Lett. **102**, 243105 (2013); 10.1063/1.4811497

[Thermal stability and electrical conductivity of multiwalled carbon nanotube \(MWCNT\)/polymethyl methacrylate \(PMMA\) nanocomposite prepared via the coagulation method](#)
AIP Conf. Proc. **1455**, 212 (2012); 10.1063/1.4732494

[Enhanced electrical and dielectric properties of graphite based PVA nanocomposite at low percolation threshold](#)
AIP Conf. Proc. **1447**, 353 (2012); 10.1063/1.4710025

[Tunneling resistance and its effect on the electrical conductivity of carbon nanotube nanocomposites](#)
J. Appl. Phys. **111**, 093726 (2012); 10.1063/1.4716010

[Effects of silica particles on the electrical percolation threshold and thermomechanical properties of epoxy/silver nanocomposites](#)
Appl. Phys. Lett. **99**, 043104 (2011); 10.1063/1.3615690

High-Voltage Amplifiers

- Voltage Range from $\pm 50\text{V}$ to $\pm 60\text{kV}$
- Current to 25A

Electrostatic Voltmeters

- Contacting & Non-contacting
- Sensitive to 1mV
- Measure to 20kV



ENABLING RESEARCH AND
INNOVATION IN DIELECTRICS,
ELECTROSTATICS,
MATERIALS, PLASMAS AND PIEZOS



www.trekinc.com

TREK, INC. 190 Walnut Street, Lockport, NY 14094 USA • Toll Free in USA 1-800-FOR-TREK • (t):716-438-7555 • (f):716-201-1804 • sales@trekinc.com

Anomalous decrease of the specific heat capacity at the electrical and thermal conductivity percolation threshold in nanocomposites

B.-W. Kim, S.-H. Park, and P. R. Bandaru^{a)}

Program in Materials Science, Department of Mechanical Engineering, University of California, San Diego, La Jolla, California 92093, USA

(Received 22 September 2014; accepted 14 December 2014; published online 24 December 2014)

We report an unusual specific heat variation in nanotube/polymer composites, related to a reduction in its value at the electrical and the thermal conductivity percolation threshold, with a concomitant increase in the crystallinity. The reduction has been interpreted in terms of the partition of the total number of nanostructures into isolated or clustered/connected entities, the numbers of which vary as a function of the nanotube filler fraction, and the consequent modulation of the entropic characteristics as well as the conductivity. © 2014 AIP Publishing LLC. [<http://dx.doi.org/10.1063/1.4905133>]

The placement of nanostructure fillers in polymers, in addition to the technological value,¹ yields significant insights into material interactions and consequent physical and chemical property modulation. A related aspect concerns the widespread use of carbon nanotube (CNT) additives in battery electrodes and polymers for composite synthesis,^{2,3} based on the advantages of a large length to diameter aspect ratio ($A.R.$). Consequently, a significant change of the composite character at relatively low (<0.01 wt. %) nanotube filler concentrations may be obtained. The underlying mechanism for the drastic change is the encompassing of the polymer matrix, through the percolation^{4,5} of the nanotubes, which has been shown to modulate the mechanical characteristics⁶ as well as significantly alter the electrical^{7,8} and thermal conductivity⁹ attributes of the polymer. Here, we report an unusual specific heat variation in nanotube/polymer composites, related to a reduction in its value at the electrical and the thermal conductivity percolation threshold, with concomitant increase in the crystallinity.

In this study, multi-walled CNTs of $A.R. \sim 35$ (estimated through the ratio of the average length $1.6 \mu\text{m}$ and diameter of 45 nm —with a standard deviation of $0.5 \mu\text{m}$ and 14 nm , respectively) were uniformly dispersed into a RET (reactive ethylene terpolymer) matrix in a volume fraction (ϕ) range of 0.004–0.1. The upper limit of ϕ was dictated by the mechanical stability of the composites, as it was found that higher ϕ made the samples brittle. The dispersion homogeneity was monitored through scanning electron microscopy (SEM) micrographs and quantified through an image processing algorithm, which allowed the comparison of the obtained uniformity with that of a preferred pattern as previously reported by our group¹⁰ (also see Sec. I in supplementary material²⁹). The rationale for the choice of the RET and further details on the processing have also been previously reported.¹¹

The electrical conductivity (σ) of the composites (with sputtered Ti (5 nm)/Au (100 nm) contacts) with electrical resistance, $R_{el} < 1 \text{ G}\Omega$ was measured through standard four-probe techniques, while for composites with $R_{el} > 1 \text{ G}\Omega$,

two-point methods were employed (using the Agilent 1500 A semiconductor device analyzer, with triaxial probes). The results, shown in Figure 1, indicate a percolation-like behavior with more than a ten order of magnitude change in the σ with increasing ϕ . We predicted^{7,12} a value of 0.021 for the percolation threshold volume fraction (ϕ_c)—per Eq. (1) below, using for the constant B a value of 1.4, appropriate for thin rods¹³

$$\phi_c(A.R.) = \frac{B}{\frac{4\pi}{3} + 2\pi(A.R.) + \frac{\pi}{2}(A.R.)^2} \left[\frac{\pi}{6} + \frac{\pi}{4}(A.R.) \right]. \quad (1)$$

A ϕ_c of ~ 0.02 was experimentally estimated through fitting the conductivity variation, very close¹⁴ to and above ϕ_c , to a power law expression of the form: $\sigma \sim |\phi - \phi_c|^t$, where t is a critical exponent.^{4,15} While the threshold could depend on microscopic details, the t would be material independent and universal¹⁶ at $t = 2$.

Concomitantly, we measured the thermal conductivity (κ) of the polymer nanocomposites through both a 3ω based

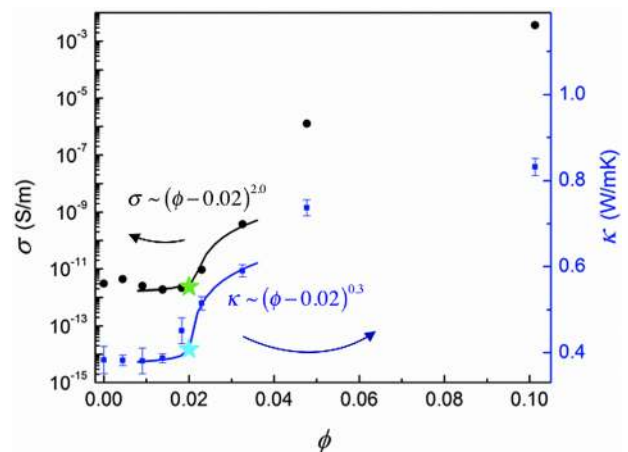


FIG. 1. Electrical and thermal conductivity percolation in the nanocomposites. The measured electrical conductivity (σ): left vertical axis, and thermal conductivity (κ): right vertical axis, as a function of the nanotube filler fraction (ϕ). The solid lines are fits to the conductivity variation near the percolation threshold ($\phi_c \sim 0.02$) to a power law expression of the form: $|\phi - \phi_c|^t$, where t is a critical exponent.

^{a)}Email: pbandaru@ucsd.edu

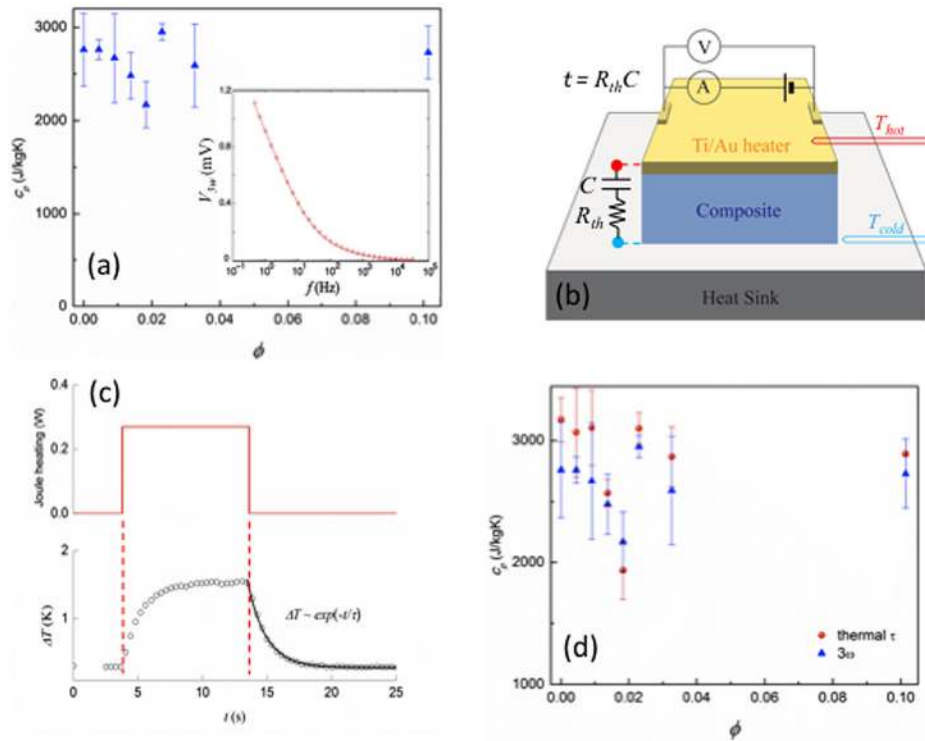


FIG. 2. (a) The variation of the C_p with ϕ , as measured by the 3ω method indicated a decrease near the ϕ_c . The inset shows the measured $V(3\omega)$, as a function of the frequency ($f = \omega/2\pi$). (b) Schematic of a thermal time constant based method for the determination of the C_p , where the temperature decay time constant $\tau = R_{th}C$ denotes the equivalent thermal resistance (R_{th}) and capacitance ($C = mC_p$), with m as the mass of the sample) estimated through a (c) fit to the thermal profile (bottom) developed in response to an application of a power pulse (top) to the Ti/Au electrodes. (d) Superposed values of C_p determined through both the 3ω and the thermal time constant based measurements clearly show a dip near ϕ_c .

methodology¹⁷ and steady state techniques. It was seen that the κ variation with ϕ also followed a percolation-like transition, and was fitted to a power law expression with a similar ϕ_c of ~ 0.02 albeit with an exponent, t of ~ 0.3 . The difference in the t from the value obtained from the electrical conductivity measurements was ascribed to the substantial influence of the interfacial resistance⁹ as well as the different physical origin of thermal transport.^{14,15} In both the electrical and thermal measurements, it was ensured that the sample and the metal lines were electrically isolated/ mutually insulated at all CNT concentrations through monitoring the electrical capacitance. While the traditional use of the 3ω method, with reference to the measured third harmonic of the voltage $V(3\omega)$, at a given angular frequency $\omega (=2\pi f$, where f is the measurement frequency)—due to the product of the alternating current: $I(\omega)$ and the Joule heating induced resistance variation: $R(2\omega)$, has been in the measurement of the κ , we coopted the underlying principles for the estimation of the specific heat capacity: C_p , of the composites. It was previously¹⁷ shown that

$$V(3\omega) = \frac{[V(\omega)]^3}{\kappa 2\pi l R_{me}^2} \frac{dR_{me}}{dT} \int_0^\infty \frac{\sin^2(kb)}{(kb)^2 \sqrt{k^2 + 2\omega\rho C_p/\kappa}} dk. \quad (2)$$

For our measurements, $l (=10 \text{ mm})$ and $2b (=70 \mu\text{m})$ refer to the length and width of the metal (me) line, which served as both the heater and thermometer and were chosen so as to approximate a narrow line heat source (with a ratio of the sample thickness to the metal line width of ~ 30). The composite density (ρ), the metal line resistance (R_{me}) as well as the related temperature coefficient ($= \frac{dR_{me}}{dT}$) was measured and calibrated. The variation of the $V(3\omega)$ over a range of f (from 0.1 Hz to 1000 Hz) was measured using a lock-in amplifier (Stanford Research Systems: SRS 830) in concert

with a Wheatstone bridge setup (used to cancel the lower voltage harmonics). In a lower range of frequencies (from 1 Hz to 100 Hz), the slope of the $V(3\omega)$ vs. $\ln(f)$ was used to deduce the κ , with P/l as the power per unit length. Such a method was employed on a variety of samples for calibration and typically yielded values within 5% of the reported results in literature (also see Sec. II in supplementary material²⁹). Subsequently, with the obtained values of κ for a given ϕ , for the nanocomposite, the C_p was estimated through a numerical solution of Eq. (2) and a fit to the entire curve: see inset to Figure 2(a). The results of the C_p variation for a range of ϕ in the nanotube/polymer composite samples are indicated, in Figure 2(a). The accuracy of estimation was determined to be $\sim 3\%$ through comparison with standards.⁹ It was noted that the observed variation was unusual in that there seemed to be a dip in the C_p magnitude close to/at the ϕ_c .

As such variation was reproducible in three sets of samples, further confirmation was attempted through another independent technique. Consequently, the C_p was measured through monitoring the decay of the temperature (T) profile developed in response to the application of electrical power pulses to sputtered Ti (10 nm)/Au (100 nm) contacts on the top and bottom of the nanocomposite sample—Figure 2(b). We defined and measured a thermal time constant (τ), as the time during which the temperature of the sample decays by a factor of e (the base of the natural logarithm) from the profiles: Figure 2(c). From the relation, $\tau = R_{th}C = R_{th}mC_p$, with $R_{th} (= \Delta T/P$, the ratio of the temperature drop: ΔT , across the sample to the applied power: P) as the thermal resistance, and C as the thermal capacitance (=the product of the mass of the sample: m and the C_p) the specific heat capacity was estimated.¹⁸ The method was calibrated through testing for the C_p of a variety of materials, e.g., pyrex glass (measured $C_p = 760 \text{ J/kg}\cdot\text{K}$ vs. reported value of $750 \text{ J/kg}\cdot\text{K}$ (Ref. 19))

and typically yielded C_p values to within 2% of those reported in literature. The previously observed decrease in the C_p values was again observed in three independent sample sets, further enhancing our confidence that the characteristic at the ϕ_c was indeed typical to the nanotube/polymer composites. The combined data sets from both the (a) 3ω methodology and (b) the heat pulse method measurements are indicated in Figure 2(d). The major sources of error, could arise from the arrangement of the nanotubes within the sample. Even though care was taken to ensure identical volume fractions of the nanotube fillers, the configurations of the nanotube fillers cannot be controlled and variations may give rise to the spread in the measured values.

We sought to understand such an unexpected change in the C_p through further diagnostics on the samples using x-ray diffraction (employing the Bruker D8, operated at 40 kV, 200 mA). A corresponding degree of crystallinity (defined for polymeric materials through the ratio of the integrated intensity of the crystalline peak to that of the amorphous background²⁰) opposite to that observed in the C_p was revealed (Figure 3) and hinted that the underlying arrangement of the nanotubes in the polymer matrix could be responsible for the specific heat variation. We discuss later how the reduction in the C_p of the composite likely has its origins in the ordering of the polymer matrix. It is pertinent to note that, in the context of ethylene based polymers akin to RET, that an increasing nanocomposite crystallinity was posited to reduce the specific heat.^{21,22} The indexing of the peak positions (inset to Figure 3), observed in the diffractogram of the nanocomposite, was done to within close accord of the published patterns of the polyethylene constituents of the RET.²³ The change in the XRD patterns with increasing ϕ has been indicated (see Sec. III in supplementary material²⁹). It should be noted that the presented XRD patterns correspond to changes in the matrix crystallinity due to the filler addition and are not *per se* indicative of the nanotubes. It was intriguing to

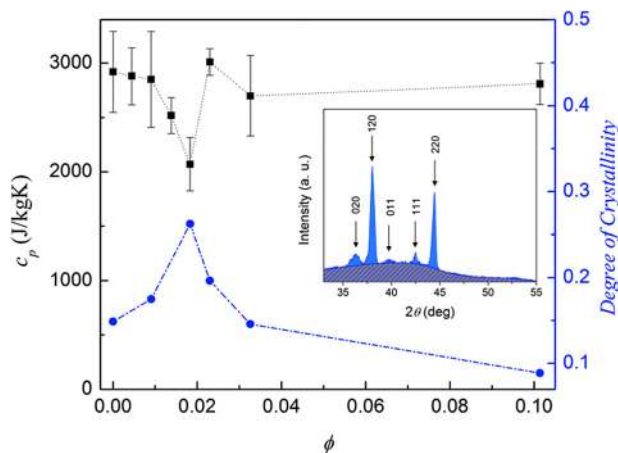


FIG. 3. Correlation of the measured specific heat capacity (C_p) to the crystallinity of the nanocomposite. The C_p (left axis) variation is anti-correlated to the degree of crystallinity (right axis). The inset indicates a typical x-ray diffractogram of the nanocomposite (for $\phi = 0.009$)—indicating the Intensity (in arbitrary units, a.u.) vs. 2θ and the crystal plane indices above the peaks, based on which the crystallinity (= the ratio of the integrated intensity of the crystalline peaks: solid to that of the total integrated area: crystalline peak + amorphous background: diagonal shaded) was determined.

consider the notion that crystallinity seems to be maximal at the nanotube percolation threshold in the polymer. While such a correlation has been previously considered for semiconductor based systems,²⁴ such as phosphorus doped Si:F:H alloys,²⁵ our work is the first report of such phenomena in nanostructure-polymer systems. The estimated degree of crystallinity of ~ 0.27 : Figure 3, at the ϕ_c was intermediate to the theoretical boundary values²⁶ of 0.15 and 0.44 for three- and two-dimensional percolating systems and indicate a tendency towards rod-like percolation,²⁷ as could be expected for nanotube containing systems.

Since ϕ_c indicates a degree of ordering, we attempted to relate a change in the configurational arrangement and entropy to the observed C_p variation. Each nanocomposite (with a different volume fraction of nanotube filler content: ϕ) can be considered a *distinct* material and would have its own C_p . It was hypothesized that the change of the C_p of a particular sample with a finite ϕ ($C_{p,\phi}$) with respect to that of the polymer alone ($C_{p,\phi=0}$) would be related to the change of nanotube organization and content (also see Sec. IV in supplementary material²⁹). It was then considered that the relative arrangement of the CNTs would determine the change as either individual entities (as at $\phi < \phi_c$) or clusters (typical at $\phi > \phi_c$). As it was previously discussed, through Figure 3, that a maximum of the degree of crystallinity corresponded to the ϕ_c , it was plausible that the connectivity of the nanotubes could be related to the observed C_p minimum. We consider the equivalence between the change of the specific heat and the change of the configurational entropy at a given temperature.²⁸ The entropic term incorporates the total number of CNTs (N_t) partitioned either into individual/isolated (N_i) or connected (N_c) constituents, i.e., $N_t = N_i + N_c$, and would be proportional to $\ln [N_t! / (N_i! N_c!)]$. The N_c refers to those nanotubes, which are mutually connected or linked at one/more locations. The argument of the logarithm would be related to the variety of possible arrangements of the N_t ($= \frac{\phi V_s}{V_{CNT}}$, where V_s and V_{CNT} represent the sample volume and that of an individual CNT—assumed to be a cylinder with mean length of 1.6 μm and diameter of 45 nm, respectively) nanostructures. We then computed the ratio of the experimentally determined specific heat values at two particular values of ϕ (say, ϕ_1 and ϕ_2), i.e., as C_{p,ϕ_1} and C_{p,ϕ_2} , referenced to the value for the polymer alone, i.e., $C_{p,\phi=0}$, through

$$\frac{(C_{p,\phi_1} - C_{p,\phi=0})}{(C_{p,\phi_2} - C_{p,\phi=0})} = \frac{\ln \left[\frac{N_{t,\phi_1}!}{N_{c,\phi_1}! (N_{t,\phi_1} - N_{c,\phi_1})!} \right]}{\ln \left[\frac{N_{t,\phi_2}!}{N_{c,\phi_2}! (N_{t,\phi_2} - N_{c,\phi_2})!} \right]}. \quad (3)$$

As the corresponding total number of nanotubes: N_{t,ϕ_1} and N_{t,ϕ_2} at ϕ_1 and ϕ_2 , respectively, are known, Eq. (3) was self-consistently solved over the range of ϕ —using C_p data from Figures 2(d) and 3, to determine the number of connected nanotubes: N_{c,ϕ_1} and N_{c,ϕ_2} at a given ϕ_1 and ϕ_2 , respectively. The results of the above computational procedure are plotted in Figure 4 and indicate an upward and a downward percolation like transition in the N_c and N_i , respectively. Such a plot seems to be in accord with the

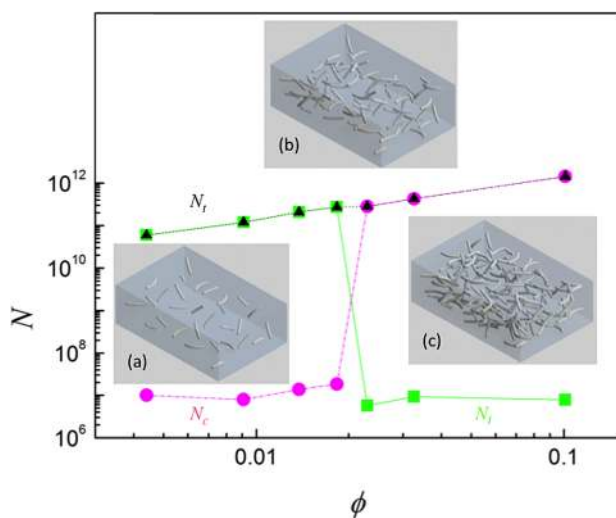


FIG. 4. The computed variation (from Eq. (3)) of the total number of CNTs (N_t) partitioned into isolated (N_i) or connected (N_c) constituents, i.e., $N_t = N_i + N_c$. The insets (a), (b), and (c) indicate plausible arrangement of the nanostructures in the polymer matrix at $\phi < \phi_c$, $\phi = \phi_c$, and at $\phi > \phi_c$, respectively. The increase in nanotube ordering with ϕ corresponds to an increase in the N_c and a decreased C_p . Further increase of ϕ beyond ϕ_c induces clustering of the N_c and an increase of the C_p .

intuition of increasing cluster formation with enhanced nanotube filler concentration. We then think that the variation of the C_p with ϕ could indeed arise from the reorganization of the nanotubes, as depicted schematically in the insets to Figure 4. The modulation of the crystallinity of the composite could arise from an initial inducement of ordering of the RET polymer matrix by the nanotubes, followed by a reduced influence at higher nanotube content due to clustering effects. Such ordering and reduced heat capacity in the polymer matrix (see Sec. IV in supplementary material²⁹) is likely the origin of the reduction in the C_p of the composite. In more detail, the increasing degree of crystallinity up to ϕ_c , facilitated through nanotube connectivity, may correspond to an enhanced ordering in the composite with a concomitant decrease in the entropy and its related C_p . In the sub-percolation threshold regime (with $\phi < \phi_c$), the nanostructures are relatively isolated and evolve to an ordered polymer matrix spanning network at $\phi \sim \phi_c$. However, further increase of the nanotube content (at $\phi > \phi_c$) leads to uneven clustering and disorder, even as N_c was increased, implying an increased C_p .

The reduction in the specific heat capacity of nanotube/polymer composites precisely near the electrical and thermal conductivity percolation threshold is remarkable in terms of thermal property modulation. It would be of much interest to explore the universal validity of the observed phenomena related to the extent to which the C_p could be diminished as a function of the nanostructure aspect ratio as well as due to

the influence of specific polymer matrix characteristics. The notion of a C_p minimum, concomitant with a κ enhancement at the ϕ_c implies an enhancement in the thermal diffusivity ($D = \kappa/\rho C_p$). It is suggested that composite materials should be synthesized with a volume fraction of fillers heat dissipation media.

This work was partially supported by a grant (CMMI 1246800) from the National Science Foundation.

- ¹S. Thomas, K. Joseph, S. K. Malhotra, K. Goda, and M. S. Sreekala, *Polymer Composites* (Wiley-VCH, Weinheim, Germany, 2013).
- ²M. F. L. De Volder, S. H. Tawfik, R. H. Baughman, and A. J. Hart, *Science* **339**, 535 (2013).
- ³R. H. Baughman, A. A. Zakhidov, and W. A. de Heer, *Science* **297**, 787 (2002).
- ⁴S. Kirkpatrick, *Rev. Mod. Phys.* **45**, 574 (1973).
- ⁵G. Ambrosetti, C. Grimaldi, I. Balberg, T. Maeder, A. Danani, and P. Ryser, *Phys. Rev. B* **81**, 155434 (2010).
- ⁶J. N. Coleman, U. Khan, W. J. Blau, and Y. K. Gun'ko, *Carbon* **44**, 1624 (2006).
- ⁷S. Pfeifer, S. H. Park, and P. R. Bandaru, *J. Appl. Phys.* **108**, 24305 (2010).
- ⁸W. Bauhofer and J. Z. Kovacs, *Compos. Sci. Technol.* **69**, 1486 (2009).
- ⁹B.-W. Kim, S.-H. Park, R. S. Kapadia, and P. R. Bandaru, *Appl. Phys. Lett.* **102**, 243105 (2013).
- ¹⁰S. Pfeifer and P. R. Bandaru, *Mater. Res. Lett.* **2**, 166 (2014).
- ¹¹S.-H. Park, P. Theilmann, P. Asbeck, and P. R. Bandaru, *IEEE Trans. Nanotechnol.* **9**, 464 (2010).
- ¹²I. Balberg, C. H. Anderson, S. Alexander, and N. Wagner, *Phys. Rev. B* **30**, 3933 (1984).
- ¹³A. Celzard, E. McRae, C. Deleuze, M. Dufort, G. Furdin, and J. F. Mareche, *Phys. Rev. B* **53**, 6209 (1996).
- ¹⁴B. I. Shklovskii and A. L. Efros, in *Electronic Properties of Doped Semiconductor* (Springer-Verlag, New York, NY, 1984).
- ¹⁵D. Stauffer and A. Aharony, *Introduction to Percolation Theory* (CRC Press, Boca Raton, FL, 1994).
- ¹⁶S. Vionnet-Menot, C. Grimaldi, T. Maeder, S. Strassler, and P. Ryser, *Phys. Rev. B* **71**, 64201 (2005).
- ¹⁷D. G. Cahill, *Rev. Sci. Instrum.* **61**, 802 (1990).
- ¹⁸R. J. Schutz, *Rev. Sci. Instrum.* **45**, 548 (1974).
- ¹⁹D. R. Lide, *CRC Handbook Chemistry and Physics*, 85th ed. (BocaRaton, FL, 2004).
- ²⁰H. Koerner, G. Price, N. A. Pearce, M. Alexander, and R. A. Vaia, *Nat. Mater.* **3**, 115 (2004).
- ²¹B. Wunderlich, *J. Chem. Phys.* **37**, 1203 (1962).
- ²²G. D'Angelo, G. Tripodo, G. Carini, A. Bartolotta, G. Di Marco, and G. Salvato, *J. Chem. Phys.* **109**, 7625 (1998).
- ²³E. R. Walter and F. P. Reding, *J. Polym. Sci.* **21**, 561 (1956).
- ²⁴I. Balberg, D. Azulay, D. Toker, and O. Millo, *Int. J. Mod. Phys. B* **18**, 2091 (2004).
- ²⁵R. Tsu, *Appl. Phys. Lett.* **40**, 534 (1982).
- ²⁶H. Scher, *J. Chem. Phys.* **53**, 3759 (1970).
- ²⁷J. Gonzalez-Hernandez, D. Martin, S. S. Chao, and R. Tsu, *Appl. Phys. Lett.* **44**, 672 (1984).
- ²⁸H. B. Callen, *Thermodynamics* (John Wiley, Inc., New York, 1960).
- ²⁹See supplementary material at <http://dx.doi.org/10.1063/1.4905133> for (i) the constitution of the RET polymer and representative SEM images of the composites, (ii) details related to the experimental determination of the thermal conductivity, (iii) representative x-ray diffractograms of the composites, and (iv) correlation of crystallinity to specific heat.